Pellet Ablation in Plasmas with a High Level of Additional Power

V. Waller, B. Pégourié, A. Géraud, G. Granata, V. Bergeaud, R. Dumont,
F. Imbeaux, V. Basiuk, L.-G. Eriksson, L. Garzotti[#]

Association Euratom-CEA sur la Fusion Contrôlée, C. E. Cadarache
F- 13108 Saint-Paul-Lèz-Durance
[#]Consorzio RFX, Corso Stati Uniti 4, I-35127 Padova

Implementation of high performance scenarios requires simultaneously a high level of additional power and a tight control of the recycling, which implies a suitable fuel supplying method like cryogenic hydrogen pellet injection. The fuelling efficiency of such a system, which is a key parameter for optimizing and interpreting the experiments, depends on both the pellet poloidal launching location and ablation profile. For these reasons, it is important to have at one's disposal a reliable modeling of the ablation process accounting for the fast ion and electron populations resulting from additional heating or current drive. Up till now, a number of models predicting the ablation rate in quasi-Maxwellian plasmas have been available. However the interaction of a pellet with fast particles was not yet treated and tested at the same level. Using realistic superthermal distributions for ions (Ion Cyclotron Resonance Heating) as well as for electrons (Lower Hybrid Current Drive), the aim of this work is to describe such a modeling scheme and to present a comparison of the numerical predictions with experimental results.

Model description

The structure of the ablation code HPI (Hydrogen Pellet Injection) is identical to that of the Neutral Gas and Plasma Shielding code described in ref.[1]. Close to the pellet surface, the ablated material is deposited in a neutral cloud where expansion is spherically symmetric. At some distance from the pellet, the cloud becomes ionized and expands essentially along the magnetic field lines (hereafter, this ionized part of cylindrical shape is referred to as "plasmoid"). At the plasmoid-plasma interface, an electrostatic sheath develops, ensuring zero net current. (The expressions derived by Emmert *et al*., [2], are used for the plasma heat and particle fluxes at the sheath entrance.) The potential distribution in the sheath and the perturbed electron and ion distributions at the plasmoid surface are calculated following ref.[3], accounting for energetic particles shining through the ionized cloud. The plasmoid characteristics (size, volume-averaged density, temperature and ionization degree), which depend strongly on the power deposited by the plasma energy carriers, are obtained from a MHD volume-averaged model [4]. (Due to the relatively small length of the plasmoid, the cross-field heat transfer through its lateral surface is generally negligible, and the heat source can be estimated from stopping-length calculations). As soon as high energy ions and electrons are considered (whose orbit dimensions are equal or larger than those of the plasmoid), the particle entry into the ionized cloud no longer remains essentially limited to the ends of the cylinder and one must account for the actual path they have to cover before reaching the pellet. For fast populations, whereas the effective surface the particles intercept increases, the shielding of the cloud decreases, both effects yielding an increase of the heat flux at the pellet surface. In the calculation of the neutral cloud hydrodynamics [5], the shape of the electron and ion distributions (altered by the crossing through the plasmoid) is

explicitly taken into account. In what concerns ice vaporization, even the most energetic ions deposit all their energy in a very thin layer close to the pellet surface, but electrons with high enough energy (with respect to the bulk of the distribution) penetrate deeply into the ice, heating the whole pellet. It is then not possible to assume that ice vaporization is a steady-state process, in equilibrium with local pellet and plasma parameters, and one must consider the whole time-history of the pellet path through the plasma to calculate the space distribution of energy in the ice and the instantaneous ablation rate. When the amount of energy deposited in the ice reaches the binding energy of the lattice, the whole pellet vaporizes. In the course of this process, the primary electrons, penetrating into the ice, loose a significant amount of their energy by ionizing H_2 molecules, creating a number of H_2^+ ions and secondary electrons [6]. The system recombines in such a way that the supernumerary electrons (of number equal to that of primary electrons that loose all their energy in the pellet) are confined at the pellet surface (which minimizes the electrostatic energy) where they are quickly eliminated. There is therefore no significant electric charge in the pellet volume and electrostriction phenomenon does not play a significant role in the vaporization process.

The inputs of the HPI code are the pellet mass, velocity and launching point (equatorial plane, low field side in the simulations presented here), the plasma geometry, pre-pellet density profile and the electron and ion distributions (energy and pitch-angle) as a function of the location inside the plasma. With regard to the comparison between the code predictions and the experimental results, 3D distribution functions have been calculated using the Monte-Carlo code FIDO [7] for the ions (ICRH – minority regime) and two fully relativistic Fokker-Planck codes for the electrons (LHCD), with different approximations in what concerns the wave absorption. The first one includes turbulence driven radial diffusion of fast electrons and a model based upon the LH propagation domain to describe the wave deposition [8] for the positive part of the LH launched spectrum. The second is coupled to a ray-tracing calculation (code DELPHINE, ref.[9]) and uses the whole launched spectrum.

Comparison with experiments

Quasi-Maxwellian plasmas (ohmic discharges)

For ohmic plasmas, the HPI code has been tested on more than 40 well-documented pellet discharges from Tore Supra, TFTR and FTU, selected in the IPADBASE (International Pellet Ablation DataBASE) [10]. The range of pellet parameters are: particle content $0.1<N_p<1.5\times10^{21}$ atoms, velocity $0.6<V_p<3$ km/s, normalized penetration $0.4<\lambda_p/a<1$ (where a is the plasma minor radius). The corresponding plasma parameters at the end of the pellet path are: $10^{19}<n_e(\lambda_p)<1.5\times10^{20}$ m^{-3} for the density and $1<T_e(\lambda_p)<4.6$ keV for the temperature. The code predictions reproduce the experimental penetrations within ±10%, i.e. with the same accuracy as what was done by previous models (e.g. [1]).

Plasmas with fast ion tail (ICRH)

For ICRH plasmas, Tore Supra data have been used. In the simulations presented in Table 1, the resonance is located at a major radius R=2.57 m and the fast ion tail becomes significant at 0.52 m from the plasma edge (this value to be compared with the measured λ_p). For the different situations investigated, the numerical simulations are in good agreement with both the experimental penetrations and main features of the ablation profiles. The comparison of pellets TSn°14153 and TSn°14143 and of pellets TSn°24854 and TSn°24846 illustrates the fact that the two main parameters governing the enhanced ablation by fast ions are the concentration of the minority species, $<n_H/n_e>$ and the injected power, P_{ICRH}.

TS n°	N_p (10^{21} at.)	V_p (km/s)	$\langle n_H/n_e \rangle$ (%)	P_{ICRH} (MW)	$n_e(\lambda_p)$ (10^{19} m^{-3})	$T_e(\lambda_p)$ (keV)	λ_p^{exp} (m)	λ_p^{ICRH} (m)	λ_p^{Ω} (m)
14153	2.8	2.3	5	2.4	4.2	2.6	0.48	0.50	0.60
14143	2.8	2.3	10	2.4	4.9	3.2	0.56	0.58	0.60
24854	2.0	3.2	6	2.3	4.9	2.5	0.72	0.74	-
24846	1.7	3.5	5	3.9	4.6	2.5	0.52	0.51	0.98

Table 1: *Comparison between experiments and code predictions for ICRH plasmas.*

A parametric study has been done with fixed plasma density and pellet parameters: $n_e(0)=5\times10^{19}$ m^{-3}, $N_p=2.5\times10^{21}$ atoms and $V_p=3$ km/s. The ohmic penetrations are $\lambda_p^{\Omega}=0.75$ m for $T_e(0)=3$ keV and $\lambda_p^{\Omega}=0.48$ m for $T_e(0)=5$ keV. The dependence of $\lambda_p^{ICRH}/\lambda_p^{\Omega}$ on $\langle n_H/n_e \rangle$ and P_{ICRH} is shown in Figure 1. At fixed value of P_{ICRH}, the ratio $\langle n_H/n_e \rangle$ determines the maximum energy of the fast ions. The pellet penetration λ_p^{ICRH} recovers its unperturbed value λ_p^{Ω} when the fast ions are stopped before they reach the pellet surface (fig.1a), for values of the ratio $\langle n_H/n_e \rangle$ down to 8 % with the parameters listed above, since the more numerous the minority species, the lower their energy. For a given value of $\langle n_H/n_e \rangle$, the injected power governs the density of the fast tail. For $P_{ICRH} \geq 8$ MW, the pellet stops as soon as it enters the region where the fast ion tail is significant. For lower values, ablation is less efficient and the pellet penetrates deeper (fig.1b). With increasing electron temperature (from 3 to 5 keV, fig.1b), the bulk plasma governs the ablation and penetration tends to be closer to ohmic calculation as long as the region where fast ion energy becomes significant is not reached.

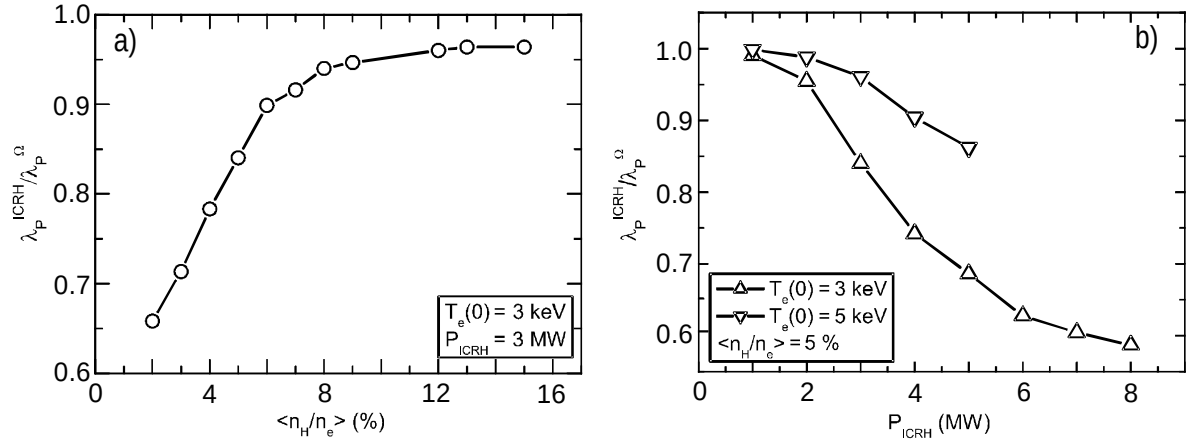

Figure 1: *Dependence of $\lambda_p^{ICRH}/\lambda_p^{\Omega}$ on $\langle n_H/n_e \rangle$ and P_{ICRH}.*

Plasmas with fast electron tail (LHCD)

The ability for the model to reproduce pellet penetrations in LHCD discharges has been tested on a standard Tore Supra scenario, with parameters (shot TSn°12583) $\langle n_e \rangle=1.9\times10^{19}$ m^{-3}, $N_p=3\times10^{20}$ atoms, $V_p=3.2$ km/s, $V_{loop}=0.2$ V and $P_{LH}=2$ MW. When using ref.[8], the value of the diffusion coefficient of fast electrons, $D(v_{//})$, is adapted to reproduce the experimental penetration. The behavior of $\lambda_p^{LHCD}/\lambda_p^{\Omega}$ with $D(v_{//}=v_{th})$ is shown in fig.2a and a good agreement is obtained between the calculated (full line) and measured (dotted line) relative penetrations for $D(v_{//}=v_{th}) \approx 0.16 \pm 0.03$ m^2s^{-1}, where v_{th} is the thermal velocity. This appears somewhat high in comparison to what is given for Tore Supra in ref.[11]. For comparison, $\lambda_p^{LHCD}/\lambda_p^{\Omega}$ calculated with the code DELPHINE [9] is also displayed (plain star). In this case, $D(v_{//})=0$ and the agreement between the calculated and measured values is due to the interaction between the negative and positive parts of the LH launched power spectrum.

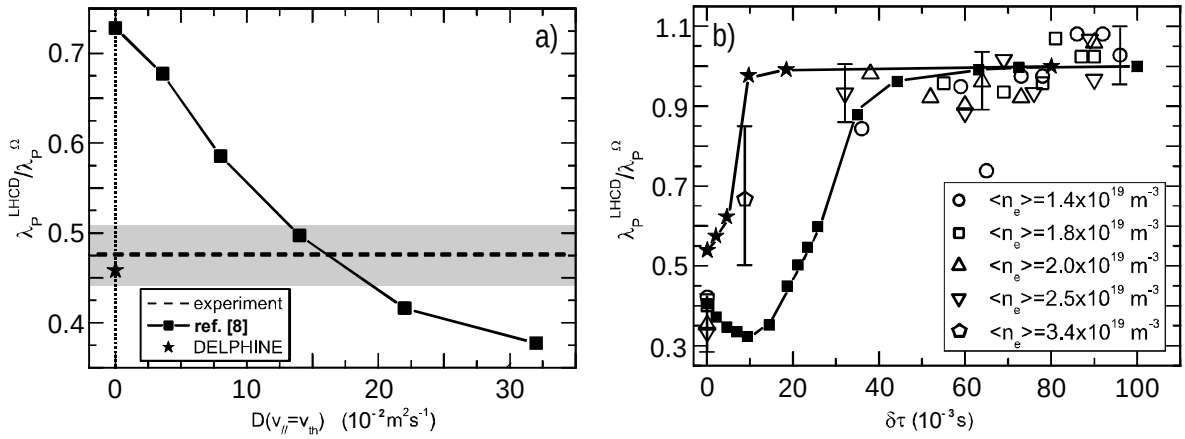

Figure 2: *Dependence of $\lambda_p^{ICRH}/\lambda_p^{\Omega}$ on $D(v_{//}=v_{th})$ and $\delta\tau$.*

For notched scenarios [12], used to recover a sufficient penetration in current drive experiments, it is the delay $\delta\tau$ between the power switch-off and the pellet injection time that governs the penetration (the other parameters being fixed). The experimental behavior of $\lambda_p^{LHCD}/\lambda_p^{\Omega}$ with $\delta\tau$ is displayed on fig.2b for pellets of velocity V_p=0.6 km/s and different plasma densities (open markers). In the different cases, when the LH power is switched-on, $\lambda_p^{LHCD} \lesssim \lambda_p^{\Omega}/2$ and the ohmic penetration is recovered at $\delta\tau \approx 20$ ms. This value seems the best compromise between current drive efficiency and pellet penetration in the frame of these experiments ($V_{loop} \neq 0$) and compares reasonably with code predictions using a constant V_{loop}. Nevertheless, a more detailed comparison between data and code predictions seems to indicate: -1- that the number of fast electrons at the plasma edge is larger than what is simulated with the code DELPHINE and -2- that assuming $D(v_{//}=v_{th}) \approx 0.16$ $m^2 s^{-1}$ in ref.[8] allows to reproduce the experimental penetration at $\delta\tau=0$ but is too high to fit the time dependence of $\lambda_p^{LHCD}/\lambda_p^{\Omega}$ on $\delta\tau$. One can also note that for the shortest $\delta\tau$'s, the ratio $\lambda_p^{LHCD}/\lambda_p^{\Omega}$ given through ref.[8] begins to decrease owing to the competition between the scattering of the fast particles in the velocity space [13] and cross-field diffusion, which causes a transient increase of the superthermal tail after the power switch-off. When considering this work, one must keep in mind that LH modeling is still an open subject (see ref.[14] for a review) and that, in the present status of the art, pellet ablation modeling is under no circumstances a means of comparison between the different LH models.

References:

[1] L. Garzotti, B. Pégourié, A. Géraud *et al.*, Nucl. Fus. **37** (1997) 1167
[2] G. A. Emmert, Phys. Fluids **23** (1980) 803
[3] L. L. Lengyel, V. A. Rozhanskij, I. Yu. Veselova, Nucl. Fus. **36** (1996) 1679
[4] L. L. Lengyel, Phys. Fluids **21** (1978) 1945
[5] S. L. Milora, C. A. Foster, IEEE Trans. Plasma Sci. **PS-6** (1978) 578
[6] F. Bottiglioni, J. Coutant, M. Fois, Phys. Rev. A **6** (1972) 1830
[7] J. Carlsson, T. Hellsten, L.-G. Eriksson, in *Proceedings of the Joint Varenna Lausanne Workshop on «Theory of Fusion Plasmas» 1994*, Compositori, Bologna (1994) 351
[8] R. Dumont, G. Giruzzi, E. Barbato, Phys. Plasmas **7** (2000) 4972
[9] F. Imbeaux, Report EUR-CEA-FC-1679 (1999)
[10] L. R. Baylor, A. Géraud, W. A. Houlberg *et al.*, Nucl. Fus. **37** (1997) 445
[11] Y. Peysson, Plasma Phys. Contr. Fusion **35** (1993) B53
[12] A. Géraud, C. A. Foster, B. Pégourié *et al.,* 19th EPS Innsbruck 1992, **Vol.16C Part I**, EPS (1992) 159
[13] G. Giruzzi, J.-L. Ségui, T. Dudok de Wit *et al.*, Phys. Rev. Lett. **74** (1995) 550
[14] Y. Peysson and TORE SUPRA Team, Plasma Phys. Control. Fusion **42** (2000) B87